Micellar Morphologies of Poly(ϵ-caprolactone)-*b*-poly(ethylene oxide) Block Copolymers in Water with a Crystalline Core

Zi-Xiu Du,† Jun-Ting Xu,*,†,‡ and Zhi-Qiang Fan†,‡

Key Laboratory of Macromolecular Synthesis and Functionalization, Department of Polymer Science & Engineering, Zhejiang University, Hangzhou 310027, China, and State Key Laboratory of Chemical Engineering, College of Materials and Chemical Engineering, Zhejiang University, Hangzhou 310027, China

Received April 27, 2007; Revised Manuscript Received July 1, 2007

ABSTRACT: The self-assembly of poly(ϵ-caprolactone)-*b*-poly(ethylene oxide) block copolymers (PCL_nPEO_{44} and PCL_nPEO_{113}) with narrow polydispersity in aqueous medium was studied using transmission electron microscopy. In this system, the formed micelles are composed of a crystalline PCL core and a soluble PEO corona. We demonstrated that the PCL-*b*-PEO block copolymers can form micelles with abundant morphologies, depending on the lengths of the blocks and composition. It is observed that for PCL_nPEO_{44} the micellar morphology changes from spherical, rodlike, wormlike, to lamellar, as the length of the PCL block increases. In contrast, most of PCL_nPEO_{113} ($n = 21-147$) block copolymers form spherical micelles, and only $PCL_{232}PEO_{113}$ exhibits mixed spherical and lamellar micellar morphologies. The effect of microstructure on micellar morphology was semiquantitatively interpreted in terms of reduced tethering density ($\tilde{\sigma}$). It is found that lamellar micelles are formed when $\tilde{\sigma}$ is smaller than a critical value of between 3.0 and 4.8. A larger $\tilde{\sigma}$ indicates crowding of the tethered chain, and spherical micelles tend to be formed.

Introduction

It is well-known that amphiphilic copolymers in a selective solvent can self-assemble into micelles when the concentration is above the critical micelle concentration (cmc). Micelles with various shapes such as spherical, cylindrical, wormlike, and vesicle micelles have been reported.[1−17] Compared with the numerous literatures about micelles of coil−coil block copolymers, the micelles of crystalline−coil block copolymers, in which the core of the micelles is crystalline, are rarely reported. The crystalline−coil micelles of block copolymers can be viewed as the solvent-soluble corona grafted on the both sides of the lamellar crystals. The grafting density is determined by the chain folding number of the crystalline block, which is related to the lengths of both blocks and crystallization temperature.[18] A longer crystalline block usually leads to a larger chain-folding number and a lower grafting density; thus, platelet (lamellar) micelles are formed,[19,20] or the large aggregates of crystals precipitate from the solution.[21−23] On the other hand, when the solvent-soluble block is long, deformation of this block may cause free energy penalty, leading to a larger chain-folding number for the crystalline block to reduce the grafting density. The long solvent-soluble block may also prevent the growth of the central lamellar crystals into large aggregates; thus, spherical and cylindrical micelles may be observed.[24,25] Moreover, the free energies of the folding surface and the lateral surface also affect the chain-folding number of the crystalline block and thus micellar morphology.[18,26] Winnik and co-workers have reported the micellar morphology of a series of crystalline poly(ferrocenylsilane)-containing block copolymers.[27−33] By changing composition, solvent, and structure of the crystalline block, spherical, cylindrical, and lamellar micelles are observed. Poly(ϵ-caprolactone)-*b*-poly(ethylene oxide) (PCL-*b*-PEO) is another crystalline−coil system. However, in most references only spherical micelles are reported for the solution of PCL-*b*-PEO in water,[34−40] and until recently vesicle, cylindrical, and wormlike micelles are observed.[41−45]

So far, the studies of micellar morphology of crystalline−coil block copolymers are scattered. There is no systematic study on the effect of microstructure of the block copolymers on the micellar morphology. In the present work, we synthesized two series of PCL-*b*-PEO block copolymers with constant PEO lengths ($M_n = 2000$ and 5000) but various PCL lengths. The self-assembly of these block copolymers in water was investigated, and the microstructures of block copolymer and micellar morphology were correlated.

Experimental Section

Materials. The poly(ϵ-caprolactone)-*b*-poly(ethylene oxide) block copolymers were synthesized by a catalyst prepared from the reaction of *N*-(2-hydroxybenzylidene)aniline with $AlEt_3$ in the presence of monomethoxypoly(ethylene oxide) ($M_n = 2000$ and $M_n = 5000$). Details of polymerization are described elsewhere.[46] The block copolymers are denoted as PCL-*b*-PEO or PCL_nPEO_{44} and PCL_nPEO_{113}, in which the subscript *n* is the polymerization degree of the PCL block, while the subscripts 44 and 113 are polymerization degrees of the PEO block, respectively. The polydispersity of the polymers was determined by GPC in a PL 220 GPC instrument with tetrahydrofuran as the eluent at 40 °C and polystyrene standards for calibration. ^{1}H NMR spectra of the polymers in deuterated chloroform solutions were recorded on a Bruker Avace-500 spectrometer with tetramethylsilane as the internal standard. The absolute number-average molecular weights of PCL-*b*-PEO block copolymers were calculated from ^{1}H NMR spectra. The molecular weight and molecular weight distribution of the PCL-*b*-PEO block copolymers are given in Table 1.

Preparation of Aqueous Solutions. The PCL-*b*-PEO block polymers were first dissolved in tetrahydrofuran (THF) to obtain a homogeneous solution at an initial concentration of 2 mg/mL. Subsequently, water was added to the polymer solutions at a rate of 1 drop every 10 s with vigorous stirring. The addition of water was continued until the water content reached 20−30 wt %,

* Corresponding author: e-mail xujt@zju.edu.cn; Tel/Fax +86-571-87952400.
† Department of Polymer Science & Engineering.
‡ College of Materials and Chemical Engineering.

10.1021/ma070977p CCC: $37.00
Published on Web 09/22/2007

Table 1. Molecular Characteristics and Micellar Sizes of PCL-*b*-PEO Block Copolymers

samples	M_n of PEO[a]	M_n[b] ($\times 10^{-3}$)	PDI	w_{PCL} (%)	micellar size (nm)
$PCL_{24}PEO_{44}$	2000	4.8	1.10	58.6	21.7 ± 5.9[c]
$PCL_{40}PEO_{44}$	2000	6.6	1.08	70.2	35.8 ± 5.5[c]
$PCL_{59}PEO_{44}$	2000	8.7	1.05	77.6	19.5 ± 2.2[d]
$PCL_{90}PEO_{44}$	2000	12.2	1.09	84.1	19.7 ± 8.4[e]
$PCL_{142}PEO_{44}$	2000	18.2	1.10	89.3	20.2 ± 5.5[e]
$PCL_{21}PEO_{113}$	5000	7.2	1.14	33.1	9.9 ± 1.1[c]
$PCL_{35}PEO_{113}$	5000	8.5	1.13	45.2	15.3 ± 2.5[c]
$PCL_{58}PEO_{113}$	5000	11.3	1.12	57.7	23.5 ± 2.9[c]
$PCL_{97}PEO_{113}$	5000	15.6	1.15	69.6	21.1 ± 3.4[c]
$PCL_{147}PEO_{113}$	5000	21.6	1.19	77.6	35.9 ± 4.3[c]
$PCL_{232}PEO_{113}$	5000	31.5	1.16	84.5	39.9 ± 13.1[c]

[a] Nominal value. [b] Evaluated by ^{1}H NMR. [c] Diameter for the spherical micelles. [d] Diameter of the cylindrical micelles. [e] Width of the lamellar micelles.

depending on the composition of the block copolymers. The resulting solutions were transferred to dialysis tubes (MWCO = 3500) and dialyzed against twice-distilled water to remove the organic solvent THF at room temperature. After dialysis, the solutions turned slightly opaque. At last, the micelle solutions were moved to a clean volumetric flask, and then a certain volume of deionized water was used to wash the dialysis bags and added to the flask to make the final polymer volume at 20.0 mL, where the calculated polymer concentration of the micelle solution series was 0.1 mg/mL.

Transmission Electron Microscopy (TEM). TEM observation was performed on a JEOL JEM-1230 electron microscope operated at an acceleration voltage of 60 kV. The samples for TEM experiments were prepared by direct dropping a small amount of the micelle solutions onto copper grids coated with carbon and then dried at atmospheric pressure at room temperature. The grids were finally negatively stained by 2 wt % phosphotungstic acid (PTA). Electron diffraction patterns were obtained directly on the dried micelles.

Results and Discussion

Morphology and Size of PCL-*b*-PEO Micelles. Figure 1 shows the TEM images of the micelles of PCL_nPEO_{44} diblock copolymers. Spherical micelles are observed for $PCL_{24}PEO_{44}$ (Figure 1a). The diameter of the micelles is 25.8 ± 2.7 nm. It is observed that spherical and short cylindrical micelles coexist in $PCL_{40}PEO_{44}$ (Figure 1b). The diameter of the spherical micelles is ca. 35.8 ± 5.5 nm. For $PCL_{59}PEO_{44}$, the long wormlike micelles are formed with a diameter of 19.5 ± 2.2 nm (Figure 1c). With further increase in the PCL block length, the micellar morphology becomes bandlike lamellae for $PCL_{90}PEO_{44}$ and $PCL_{142}PEO_{44}$ (Figure 1d,e).

Figure 2 shows the TEM images of the micelles prepared from the aqueous solutions of PCL_nPEO_{113} diblock copolymers. It can be seen that the spherical micelles are formed for all PCL_nPEO_{113} diblock copolymers, regardless of the PCL length. In the longest $PCL_{232}PEO_{113}$, sometimes lamellar micelles are observed as well (Figure 2g). For the shorter PCL_nPEO_{113} diblock copolymers, such as $PCL_{21}PEO_{113}$, $PCL_{35}PEO_{113}$, and $PCL_{58}PEO_{110}$, the sizes of the spherical micelles are uniform, while the longer $PCL_{147}PEO_{110}$ and $PCL_{232}PEO_{113}$ exhibit a broad distribution in the diameter of the spherical micelles.

Figure 3 shows the electron diffraction patterns of micelles of $PCL_{24}PEO_{44}$ and $PCL_{90}PEO_{44}$, which were obtained directly on micelles. It is found that in the dried micelles of $PCL_{24}PEO_{44}$ both PCL and PEO blocks are crystallizable. On the basis of the result reported in references,[22] we can assign the electron diffraction pattern. The inner four strong diffraction spots are attributed to the (120) plane of monoclinic PEO crystals. The weak four diffraction spots in the middle and the outer two spots correspond to the (110) and (120) reflections of orthorhombic PCL crystals, respectively. The electron diffraction pattern of the dried micelle of $PCL_{90}PEO_{44}$ indicates that the chain direction of both PCL and PEG block is parallel to the electron beam. In the electron pattern of the dried micelles of $PCL_{90}PEO_{44}$, only the diffraction of PCL crystals is observed, showing that the PEO block is noncrystalline in the micelles of this block copolymer. The electron patterns confirm that the PCL block in the core of the PCL-*b*-PEO micelles is crystalline.

Reduced Tethering Density. As can be seen from Figures 1 and 2, the micellar morphology of PCL_nPEO_{44} block copolymers changes from sphere to cylinder and then to wormlike and lamellae with increasing PCL block length, while all PCL_nPEO_{113} block copolymers exhibit spherical micellar

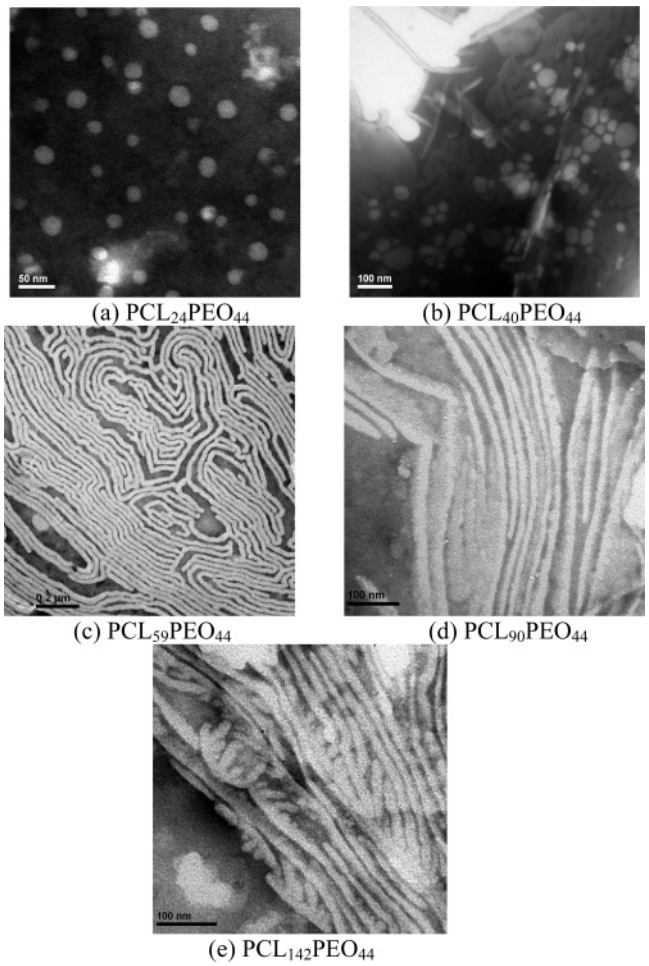

(a) $PCL_{24}PEO_{44}$ (b) $PCL_{40}PEO_{44}$ (c) $PCL_{59}PEO_{44}$ (d) $PCL_{90}PEO_{44}$ (e) $PCL_{142}PEO_{44}$

Figure 1. TEM images of micelles of PCL_mPEO_{44} block copolymers: (a) $PCL_{24}PEO_{44}$, (b) $PCL_{40}PEO_{44}$, (c) $PCL_{59}PEO_{44}$, (d) $PCL_{90}PEO_{44}$, and (e) $PCL_{142}PEO_{44}$.

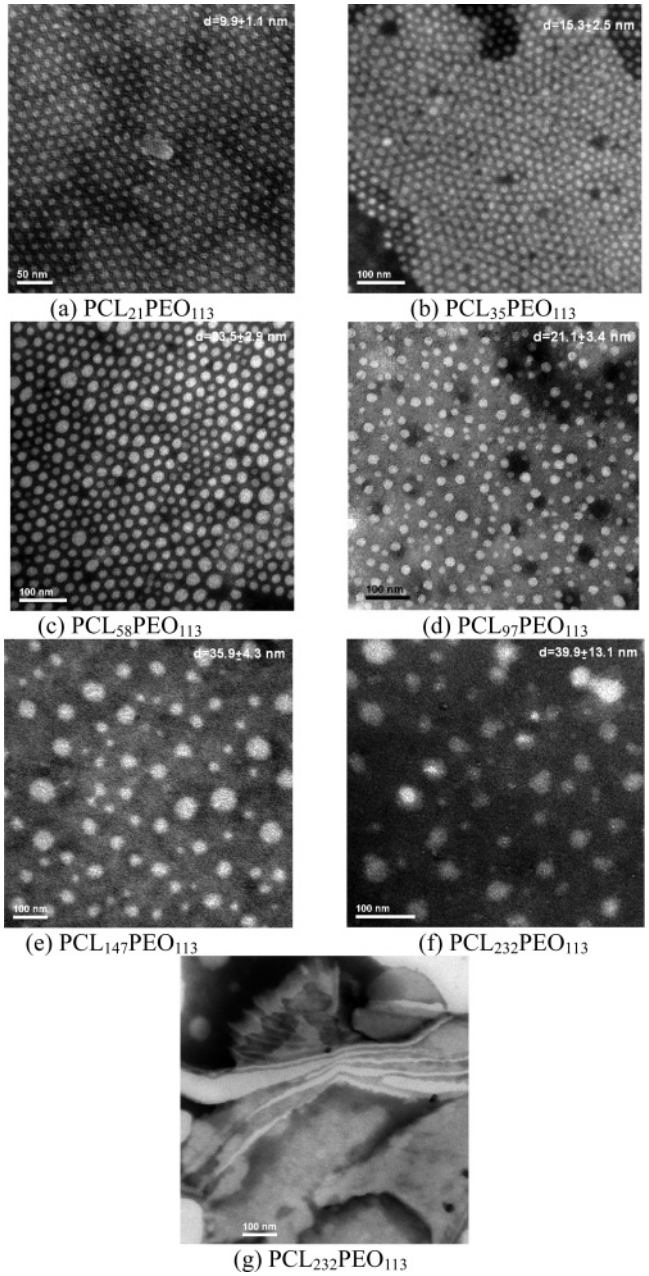

Figure 2. TEM images of micelles of PCL_nPEO_{113} block copolymers: (a) $PCL_{21}PEO_{113}$, (b) $PCL_{35}PEO_{113}$, (c) $PCL_{58}PEO_{113}$, (d) $PCL_{97}PEO_{113}$, (e) $PCL_{147}PEO_{113}$, and (f),(g) $PCL_{232}PEO_{113}$.

morphology. Therefore, the lengths of PCL and PEO blocks have an important effect on the micellar morphology. This can be qualitatively explained by Vilgis theory.[18] For the PCL_n-PEO_{113} block copolymers, the PEO block is longer, and there is a larger contribution to the overall free energy. To avoid overcrowding, spherical rather than lamellar micelles tend to be formed. On the other hand, with increase of the PCL block, the folding number of PCL increases, and thus the area occupied by each PEO chain becomes larger, leading to decrease in crowding of the tethered PEO block, and spherical micelles are gradually transformed into lamellar ones as the length of the PCL block increases.

In order to further correlate the structure of PCL-*b*-PEO block copolymer with the micellar shape, the reduced tethering density is semiquantitatively estimated. Recently, Cheng and co-workers studied the single crystals of poly(ethylene oxide)-*b*-polystyrene (PEO-*b*-PS) and poly(L-lactic acid)-*b*-polystyrene (PLLA-*b*-PS)

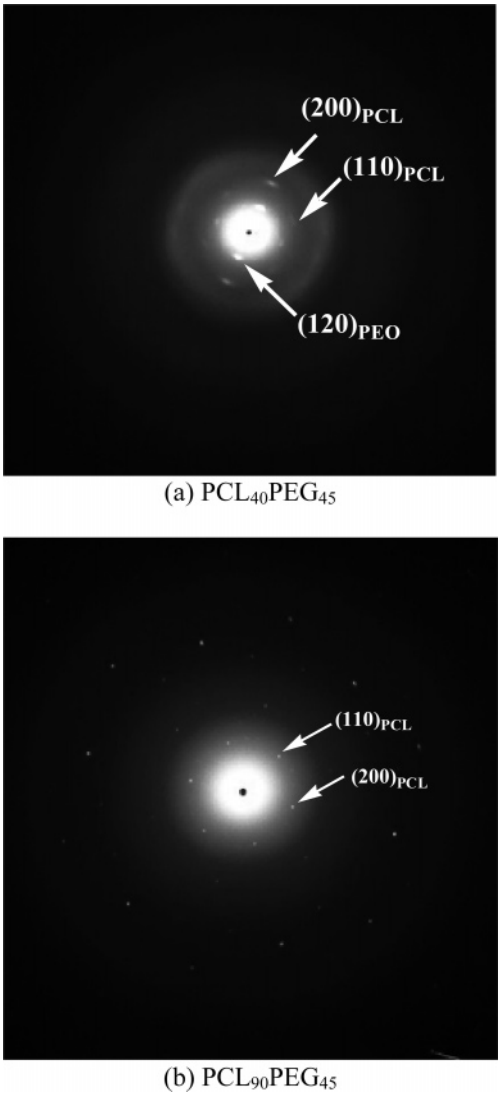

Figure 3. Electron diffraction patterns of micelles of $PCL_{24}PEO_{44}$ (a) and $PCL_{90}PEO_{44}$ (b).

grown from dilute solution.[23,47] They found that when reduced tethering density, $\tilde{\sigma}$ (which is defined by $\sigma\pi R_g^2$, where σ is the tethered chain density and is equal to the reciprocal of the area occupied by each noncrystalline chain and R_g is the radius of gyration of the tethered chain in its end-free state at the same conditions), reaches 3.7, the state of overcrowding is reached and will cause a discontinuous change in thickness of the single crystals. Here, the tethering density (σ) of PEO on the surface of PCL crystals can be calculated according to the following equation:[23]

$$\sigma = 1/S = 1/\left(\frac{2M_n^{PCL}}{N_A\rho_{PCL}l_{PCL}}\right) = \frac{N_A\rho_{PCL}l_{PCL}}{2M_n^{PCL}} \qquad (1)$$

where is S the average area occupied by each PEO chain, N_A is Avogadro's constant, ρ_{PCL} is the density of PCL crystals (ρ_{PCL}=1.20 g/cm^3), l_{PCL} is the thickness of the crystalline PCL core in the micelles, and M_n^{PCL} is the molecular weight of the PCL block. Because of the difficulty in experimental measurement of the real thickness and crystallinity of PCL crystals inside the micelles, we assume that the value of l_{PCL} is 10 nm, which is the typical thickness of polymer crystals, and the crystallinity is 100%.

Table 2. Estimated Areas Occupied by per PEO Chain (*S*) and the Reduced Tethering Density ($\tilde{\sigma}$) in the Micelles of PCL-*b*-PEO Block Copolymers

samples	M_n of PEO	S (nm^2)[a]	$\tilde{\sigma}$[b]
$PCL_{24}PEO_{44}$	2000	0.757	11.82
$PCL_{40}PEO_{44}$	2000	1.26	7.10
$PCL_{59}PEO_{44}$	2000	1.86	4.81
$PCL_{90}PEO_{44}$	2000	2.84	3.15
$PCL_{142}PEO_{44}$	2000	4.48	2.00
$PCL_{21}PEO_{113}$	5000	0.663	34.67
$PCL_{35}PEO_{113}$	5000	1.104	20.82
$PCL_{58}PEO_{113}$	5000	1.83	12.56
$PCL_{97}PEO_{113}$	5000	3.06	7.51
$PCL_{147}PEO_{113}$	5000	4.64	4.95
$PCL_{232}PEO_{113}$	5000	7.32	3.14

[a] Assuming that the thickness of PCL crystals is 10 nm, the crystallinity of the PCL block is 100%, and $\rho_{PCL} = 1.20$ g/cm^3. [b] The reduced tethering density $\tilde{\sigma} = \pi R_g^2/S$.

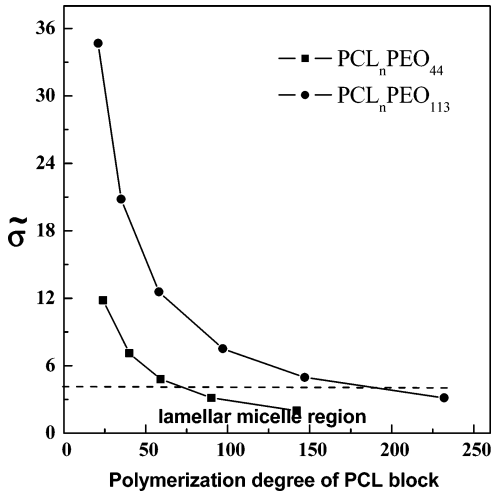

Figure 4. Changes of the reduced tethering density with the length of the PCL block in PCL_nPEO_{44} and PCL_nPEO_{113}.

The reduced tethering density $\tilde{\sigma}$ is defined as[48]

$$\tilde{\sigma} = \sigma\pi R_g^{\ 2} \tag{2}$$

where R_g^2 is the square of gyration radius of free PEO.

$$R_g = \sqrt{\langle R^2\rangle/6} = b\sqrt{N/6} \tag{3}$$

where R is the end-to-end distance of PEO and b is Kuhn length. For PEO, $b = 11$ Å and $N = M_n^{PEO}/M_0$ ($M_0 = 137$ g/mol).[49]

The estimated values of S and $\tilde{\sigma}$ are given in Table 2, and the change of $\tilde{\sigma}$ with the PCL length at a given PEO length is shown in Figure 4. As expected, the reduced tethering density decreases as the PCL block increases for both PCL_nPEO_{44} and PCL_nPEO_{113} block copolymer series. When the length of the PCL block is similar, the value of $\tilde{\sigma}$ for PCL_nPEO_{113} is far larger than that for PCL_nPEO_{44}. From Figure 1 one can see that, for PCL_nPEO_{44} block copolymers, lamellar micelles are formed when the polymerization degree of the PCL block reaches 90. The value of $\tilde{\sigma}$ corresponding to $PCL_{90}PEO_{44}$ is 3.15. For PCL_n-PEO_{113} lamellar micelles is observed in $PCL_{232}PEO_{113}$, in which the value of $\tilde{\sigma}$ is 3.14. On the other hand, the first block copolymer with nonlamellar micellar morphology is PCL_{59}-PEO_{44} in PCL_nPEO_{44} serial and $PCL_{147}PEO_{113}$ in PCL_nPEO_{113} serial, in which the values of $\tilde{\sigma}$ are 4.81 and 4.95, respectively. Therefore, we can tentatively conclude that in the crystalline−coil PCL-*b*-PEO block copolymers the critical value of $\tilde{\sigma}$ for formation of lamellar micelles is between 3.0 and 4.8. This critical value is not far from values for the onset of the tethered chain crowding.[23,47,48] When the reduced tethering density is smaller than this value, lamellar micelles may be formed. Above this critical value, micelles of other shapes are formed. The larger the reduced tethering density, the higher tendency for formation of spherical micelles. It should be noted that the critical value estimated in the present work is relatively rough and is not accurate, since in calculation of the area occupied by each PEO chain, the thickness of the PCL crystals is assumed to be 10 nm for all block copolymers and crystallinity of PCL is 100%, which is not the real situation. Moreover, the crystalline−coil micelles are not formed under state of thermodynamic equilibrium. The crystalline core of the micelles may solidify the micellar structure before it reaches thermodynamic equilibrium. The long soluble PEO block may also kinetically hinder the aggregation of PCL block, especially in PCL_nPEO_{113}. However, our result still clearly shows that the crowding of the tethering chain is the main factor responsible for the change of micellar shape in crystalline−coil PCL-*b*-PEO block copolymers.

Conclusions

The results show that the morphology of the crystalline−coil micelles of PCL-*b*-PEO block copolymers strongly depends on the lengths of both blocks. For PCL_nPEO_{44} block copolymers, spherical micelles are formed for the block copolymer with the shortest PCL block ($PCL_{24}PEO_{44}$), then the micellar morphology turns into cylindrical and wormlike as the length of the PCL block increases, and finally lamellar micelles are formed in the longest block copolymer $PCL_{142}PEO_{44}$. For PCL_nPEO_{113} block copolymers, spherical micelles are formed in all samples studied in the present work, but lamellar micelles are observed in the longest block copolymer $PCL_{232}PEO_{44}$ as well. This behavior can be explained on the basis of the reduced tethering density ($\tilde{\sigma}$). It is found that that lamellar micelles can be formed when $\tilde{\sigma}$ is smaller than a critical between 3.0 and 4.8, which indicates onset of overcrowding of the tethered PEO chains. Spherical micelles tend to be formed at a large $\tilde{\sigma}$.

Acknowledgment. This work was supported by the National Natural Science Foundation of China (20374046 and 20674073), Specialized Research Fund for the Doctoral Program of High Education (SRFDP), and the New Century Supporting Program for the Talents by Ministry of Education, China. The authors also thank Prof. Stephen Z. D. Cheng at the University of Akron for valuable discussions.

Supporting Information Available: DSC noncrystallization curves and WAXD patterns of PCL_n-*b*-PEO_{113} in the bulk and particle size distributions of PCL_nPEO_{44} micelles and PCL_nPEO_{113}. This material is available free of charge via the Internet at http://pubs.acs.org.

References and Notes

(1) Zhang, L. F.; Eisenberg, A. *Science* **1995**, *268*, 1728.
(2) Yu, Y. S.; Eisenberg, A. *J. Am. Chem. Soc.* **1997**, *119*, 8383.
(3) Cornelissen, J.; Fischer, M.; Sommerdijk, N.; Nolte, R. J. M. *Science* **1998**, *280*, 1427.
(4) Borsali, R.; Minatti, E.; Putaux, J. L.; Schappacher, M.; Deffieux, A.; Viville, P.; Lazzaroni, R.; Narayanan, T. *Langmuir* **2003**, *19*, 6.
(5) Ravenelle, F.; Marchessault, R. H. *Biomacromolecules* **2003**, *4*, 856.
(6) Liu, X. Y.; Kim, J. S.; Wu, J.; Eisenberg, A. *Macromolecules* **2005**, *38*, 6749.
(7) Bhargava, P.; Zheng, J. X.; Li, P.; Quirk, R. P.; Harris, F. W.; Cheng, S. Z. D. *Macromolecules* **2006**, *39*, 4880.
(8) Gao, Z. S.; Varshney, S. K.; Wong, S.; Eisenberg, A. *Macromolecules* **1994**, *27*, 7923.
(9) Zhang, L. F.; Eisenberg, A. *J. Am. Chem. Soc.* **1996**, *118*, 3168.

(10) Shen, H. W.; Eisenberg, A. *J. Phys. Chem. B* **1999**, *103*, 9473.
(11) Choucair, A.; Eisenberg, A. *Eur. Phys. J. E* **2003**, *10*, 37.
(12) Jain, S.; Bates, F. S. *Science* **2003**, *300*, 460.
(13) Chen, E. Q.; Xia, Y.; Graham, M. J.; Foster, M. D.; Mi, Y. L.; Wu, W. L.; Cheng, S. Z. D. *Chem. Mater.* **2003**, *15*, 2129.
(14) Bhargava, P.; Tu, Y. F.; Zheng, J. X.; Xiong, H. M.; Quirk, R. P.; Cheng, S. Z. D. *J. Am. Chem. Soc.* **2007**, *129*, 1113.
(15) Izzo, D.; Marques, C. M. *Macromolecules* **1997**, *30*, 6544.
(16) Zhang, L. F.; Eisenberg, A. *Polym. Adv. Technol.* **1998**, *9*, 677.
(17) Ding, J. F.; Liu, G. J. *Langmuir* **1999**, *15*, 1738.
(18) Vilgis, T.; Halperin, A. *Macromolecules* **1991**, *24*, 2090.
(19) Lin, E. K.; Gast, A. P. *Macromolecules* **1996**, *29*, 4432.
(20) Richter, D.; Schneiders, D.; Monkenbusch, M.; Willner, L.; Fetters, L. J.; Huang, J. S.; Lin, M.; Mortensen, K.; Farago, B. *Macromolecules* **1997**, *30*, 1053.
(21) Lotz, B.; Kovacs, A. J. *Kolloid Z. Z. Polym.* **1966**, *209*, 97.
(22) Sun, J. R.; Chen, X. S.; He, C. L.; Jing, X. B. *Macromolecules* **2006**, *39*, 3717.
(23) Zheng, J. X.; Xiong, H. M.; Chen, W. Y.; Lee, K. M.; Van Horn, R. M.; Quirk, R. P.; Lotz, B.; Thomas, E. L.; Shi, A. C.; Cheng, S. Z. D. *Macromolecules* **2006**, *39*, 641.
(24) Xu, J. T.; Fairclough, J. P. A.; Mai, S. M.; Ryan, A. J. *J. Mater. Chem.* **2003**, *13*, 2740.
(25) Xu, J. T.; Jin, W.; Liang, G. D.; Fan, Z. Q. *Polymer* **2005**, *46*, 1709.
(26) Fu, J.; Luan, B.; Yu, X.; Cong, Y.; Li, J.; Pan, C. Y.; Han, Y. C.; Yang, Y. M.; Li, B. Y. *Macromolecules* **2004**, *37*, 976.
(27) Massey, J.; Power, K. N.; Manners, I.; Winnik, M. A. *J. Am. Chem. Soc.* **1998**, *120*, 9533.
(28) Massey, J. A.; Temple, K.; Cao, L.; Rharbi, Y.; Raez, J.; Winnik, M. A.; Manners, I. *J. Am. Chem. Soc.* **2000**, *122*, 11577.
(29) Cao, L.; Manners, I.; Winnik, M. A. *Macromolecules* **2001**, *34*, 3353.
(30) Wang, X. S.; Winnik, M. A.; Manners, I. *Macromol. Rapid Commun.* **2002**, *23*, 210.
(31) Cao, L.; Manners, I.; Winnik, M. A. *Macromolecules* **2002**, *35*, 8258.
(32) Gohy, J. F.; Lohmeijer, B. G. G.; Alexeev, A.; Wang, X. S.; Manners, I.; Winnik, M. A.; Schubert, U. S. *Chem.—Eur. J.* **2004**, *10*, 4315.
(33) Guerin, G.; Raez, J.; Manners, I.; Winnik, M. A. *Macromolecules* **2005**, *38*, 7819.
(34) Ryu, J. G.; Jeong, Y. I.; Kim, I. S.; Lee, J. H.; Nah, J. W.; Kim, S. H. *Int. J. Pharm.* **2000**, *200*, 231.
(35) Nie, T.; Zhao, Y.; Xie, Z. W.; Wu, C. *Macromolecules* **2003**, *36*, 8825.
(36) Shi, B.; Fang, C.; You, M. X.; Zhang, Y.; Fu, S. K.; Pei, Y. Y. *Colloid Polym. Sci.* **2005**, *283*, 954.
(37) Park, E. K.; Lee, S. B.; Lee, Y. M. *Biomaterials* **2005**, *26*, 1053.
(38) Kim, M. S.; Hyun, H.; Cho, Y. H.; Seo, K. S.; Jang, W. Y.; Kim, S. K.; Khang, G.; Lee, H. B. *Polym. Bull. (Berlin)* **2005**, *55*, 149.
(39) Choi, C.; Chae, S. Y.; Kim, T. H.; Kweon, J. K.; Cho, C. S.; Jang, M. K.; Nah, J. W. *J. Appl. Polym. Sci.* **2006**, *99*, 3520.
(40) Lu, C. F.; Guo, S. R.; Zhang, Y. Q.; Yin, M. *Polym. Int.* **2006**, *55*, 694.
(41) Ghoroghchian, P. P.; Li, G. Z.; Levine, D. H.; Davis, K. P.; Bates, F. S.; Hammer, D. A.; Therien, M. J. *Macromolecules* **2006**, *39*, 1673.
(42) Zhang, J.; Wang, L. Q.; Wang, H. J.; Tu, K. H. *Biomacromolecules* **2006**, *7*, 2492.
(43) Geng, Y.; Discher, D. E. *Polymer* **2006**, *47*, 2519.
(44) Sachl, R.; Uchman, M.; Matejicek, P.; Prochazka, K.; Stepanek, M.; Spirkova, M. *Langmuir* **2007**, *23*, 3395.
(45) Geng, Y.; Discher, D. E. *J. Am. Chem. Soc.* **2005**, *127*, 12780.
(46) Du, Z. X.; Xu, J. T.; Yang, Y.; Fan, Z. Q. *J. Appl. Polym. Sci.* **2007**, *105*, 771.
(47) Chen, W. Y.; Zheng, J. X.; Cheng, S. Z. D.; Li, C. Y.; Huang, P.; Zhu, L.; Xiong, H. M.; Ge, Q.; Guo, Y.; Quirk, R. P.; Lotz, B.; Deng, L. F.; Wu, C.; Thomas, E. L. *Phys. Rev. Lett.* **2004**, *93*, 028301.
(48) Kent, M. S. *Macromol. Rapid Commun.* **2000**, *21*, 243.
(49) Rubinstein, M.; Colby, R. H. *Polymer Physics*; Oxford University Press: Oxford, 2003.

MA070977P